

A SIMPLE MODEL OF DRAINAGE FLOW ON A SLOPE

JUNSEI KONDO and TAKESHI SATO

Geophysical Institute, Tohoku University, Sendai, 980, Japan

(Received 27 July, 1987)

Abstract. The concept of a cold air 'Parcel' is introduced for describing the bulk properties of drainage flow. By means of a model based on the momentum and sensible heat transports under calm conditions, the thickness h and velocity u of the Parcel are derived in simple forms. It is shown that h and u correspond to the inversion height and maximum velocity of actual drainage flow. The governing parameters for h and u are the length and vertical drop of the slope, potential temperature difference between the ambient atmosphere and the Parcel, aerodynamic condition of the slope surface expressed by the mean bulk coefficients, and ambient stability. The mean bulk coefficients depend on the roughness lengths for the velocity and potential temperature profiles and are decreasing functions of the slope length.

The Parcel Model agrees qualitatively with Manins and Sawford's (1979) model under neutral ambient stratification. But agreement is not so good under stable conditions. The thickness and velocity of drainage flow predicted by the Parcel Model agree with observations on slopes several tens of meters to several hundred kilometers long.

1. Introduction

At night, cold air adjacent to an inclined ground surface descends under the force of gravity, and drainage flows develop in mountainous regions. Many investigators have described this phenomenon and have carried out observations at various places, especially in Alpine areas (Atkinson, 1981). Recently mountain and valley winds have received considerable interest in connection with the problems of transport and diffusion of air pollutants (Dickerson and Gudiksen, 1983). Drainage flow enhances momentum and sensible heat transports to the ground surface, so that energy exchange is more active on an inclined surface than on a horizontal one. As a result over a complex mountainous region, drainage flows bring cold air into basins and valleys, which intensifies cooling of the atmosphere, sometimes resulting in the development of an inland local High.

Drainage flow has been studied theoretically by two general methods. One is to make a model considering relevant physical processes (physical or hydraulic model), in which bulk properties of drainage flow are described without taking account of its internal structure. Papers by Defant (1933), Reiher (1936), Manins and Sawford (1979), Briggs (1981), and Fitzjarrald (1984) belong to this category. The other is to incorporate the turbulent transport process within drainage flow into the model (dynamic model), and to solve the governing equations analytically or numerically. The studies of Prandtl (1952), Rao and Snodgrass (1981), Yamada (1981, 1983), Garrett (1983), and Gutman (1983) belong to the latter class.

Topography and ground surface conditions are actually complex and varying from one place to another. It is important to simulate details of the drainage flow over real topography, and dynamic models are suitable for such purposes. On the other hand,

knowledge of the sensitivities of drainage flow to topographic features and to ground surface conditions is necessary for the study of energy exchange over extensive areas with complex ground surfaces.

In the present study, we develop a new physical model of the drainage flow on a plain slope by introducing the concept of the 'Parcel' which describes the properties of drainage flow, and which is useful to parameterize the energy exchange over a complex terrain. In Section 2 the principle of the Parcel Model is developed. The thickness and velocity of the Parcel, which correspond to those of actual drainage flow, are derived on the basis of momentum and sensible heat transports, and they are shown to depend on the slope length, vertical drop from the crest, potential temperature difference between the ambient atmosphere and the Parcel, aerodynamic condition of the slope surface, and ambient stability. In Section 3, some results are compared with previous works and with available observations.

2. Model of Drainage Flow on a Slope

2.1. PRINCIPLE OF THE PARCEL MODEL

The stationary drainage flow on a uniform and plain slope is described under quiet ambient wind conditions. Radiative cooling and latent heat transport are neglected.

The concept of a cold air 'Parcel' is introduced. As this Parcel descends from the top of the slope (crest), its potential temperature decreases due to the transport of sensible heat to the slope surface. The thickness and velocity of the Parcel are denoted by h and u , respectively. The potential temperature of the Parcel Θ_1 is defined by

$$\Theta_1 = \frac{\Theta + \Theta_s}{2}, \quad (1)$$

where Θ and Θ_s are the potential temperatures of the ambient atmosphere and the slope surface, respectively. This definition yields the potential temperature difference θ as

$$\Theta_1 - \Theta_s = \Theta - \Theta_1 = \theta, \quad (2)$$

which is assumed to be constant along the slope.

The Parcel is shown schematically in Figure 1, in which the slope length l and vertical drop $\delta z (= l \sin \alpha)$ are measured from the crest, and α is the slope angle. These variables are designated topographic parameters of the slope.

2.2. CASES OF NEUTRAL AMBIENT STRATIFICATION

The heat budget of the Parcel descending the slope under neutral ambient stratification is considered. Though the Parcel transports heat to the slope surface continuously during descent, it is assumed that the heat is released instantaneously to the crest surface and the Parcel descends the interval l retaining its thickness h . These assumptions are somewhat analogous to that of the mixing-length theory. The released heat per unit time

where $F_5 = \tau_h/\tau_0$. Manins and Sawford (1979) parameterized surface stress with a very small drag coefficient, and interfacial drag with an entrainment coefficient. They concluded that the interfacial drag is the dominant retarding force. Horst and Doran (1986), however, obtained a ratio of interfacial drag to surface stress (i.e., F_5) of between $1/1.2$ and $\frac{1}{3}$ from the observations and they mentioned that the relative importance of the two retarding forces is likely to change with the downslope growth of drainage flow. In this study, F_5 is assumed to be unity for simplification.

From Equations (6) and (7), the equation of motion is rewritten as

$$\frac{du}{dt} = g' \left(1 - \frac{u^2}{u_\infty^2} \right), \quad (8)$$

where

$$\left. \begin{aligned} g' &= \frac{g\theta}{\Theta_0} \sin \alpha, \\ u_\infty^2 &= \frac{g'h}{(1 + F_5)C_M}. \end{aligned} \right\} \quad (9)$$

Here u_∞ is the terminal velocity of the Parcel descending with constant thickness. By neglecting the Lagrangian time derivative in Equation (8) and with Equation (5a), an approximate expression for the velocity of the Parcel is obtained as

$$u \simeq u_\infty = \left\{ \frac{g\theta}{\Theta_0} \sin \alpha \frac{C_H}{(1 + F_5)C_M} l \right\}^{1/2}. \quad (10a)$$

It will be shown later that u corresponds to the maximum velocity, u_{\max} , of actual drainage flow.

The mean bulk coefficients, C_H and C_M , depend both on the aerodynamic roughness of the slope surface and on the slope length (see Section 2.5). If the slope-length dependence is small, Equations (5a) and (10a) indicate the following properties of the Parcel: the thickness h increases in proportion to slope length; the Parcel is thick over a rough surface slope (large C_H) and thin over a smooth one (small C_H); the velocity u increases in proportion to both the square root of the vertical drop and the square root of potential temperature difference; the velocity is large when C_H/C_M is large because of relatively small frictional force. These properties are confirmed by observations as shown in Figure 5.

2.3. CASES OF STABLE AMBIENT STRATIFICATION

When the ambient atmosphere is stably stratified as

$$\Theta(l) = \Theta(0) - \gamma \delta z, \quad (11)$$

the mean heat loss of the Parcel during descent is given by

$$\langle H_0 \rangle = \frac{c_p \rho (\theta + \gamma \delta z) h}{t}, \quad t = \frac{l}{\langle u \rangle}, \quad (3b)$$

where $\Theta(0)$ is the ambient potential temperature at the crest, and γ is the gradient of Θ .

From Equations (3b) and (4), the thickness of the Parcel is obtained as

$$h = \frac{C_H l}{1 + l/l_c}, \quad (5c)$$

where

$$l_c = \frac{\theta}{\gamma \sin \alpha} = \frac{\Theta - \Theta_1}{\gamma \sin \alpha}. \quad (12)$$

The length l_c represents the influence of ambient stability on drainage flow, and is denoted as the 'equilibrium length of slope'. When $\gamma \neq 0$, Equations (5a) and (10a) hold for the slope of $l \ll l_c$. In the case of $l \gg l_c$, the following expressions are derived:

$$h = h_c = C_H l_c \quad (\text{for } l \gg l_c), \quad (5b)$$

$$u = u_c = \left\{ \frac{g\theta}{\Theta_0} \sin \alpha \frac{C_H}{(1 + F_3) C_M} l_c \right\}^{1/2} \quad (\text{for } l \gg l_c). \quad (10b)$$

If the mean bulk coefficients do not change with slope length, the equilibrium thickness h_c and velocity u_c are constant regardless of the magnitudes of slope length and of vertical drop, respectively. They become smaller as ambient stability increases.

2.4. RELATION BETWEEN THE PARCEL AND DRAINAGE FLOW

Because the present Parcel Model does not describe the internal structure of drainage flow, the relation between the concept of the 'Parcel' and actual drainage flow is examined with the aid of some dynamic models and observations.

The characteristic thickness and velocity of drainage flow, \tilde{h} and \tilde{u} , are defined by

$$\tilde{h}(x) = \frac{1}{\theta} \int_0^{\infty} \theta'(x, z) dz, \quad (13)$$

$$\tilde{u}(x) = \frac{1}{\tilde{h}(x)} \int_0^{\tilde{h}(x)} u'(x, z) dz. \quad (14)$$

Here, θ' is the deviation of potential temperature of drainage flow from ambient

potential temperature, and u' is the velocity of the drainage flow itself. The origin of the coordinate system is located at the crest. The x -axis is taken in the downslope direction, and the z -axis normal to the slope. It is assumed that θ defined by Equation (2) is constant along the slope. The characteristics, \tilde{h} and \tilde{u} , are the integral scales of potential temperature deviation and velocity distributions, respectively, as shown in Figure 2.

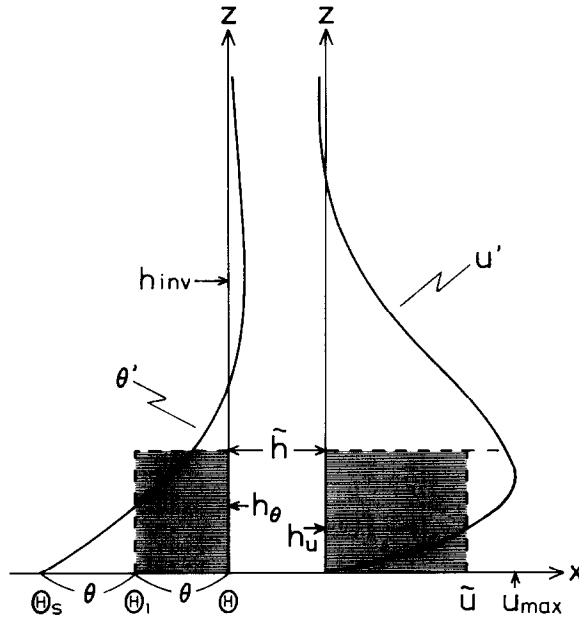


Fig. 2. Profiles of potential temperature deviation and velocity of drainage flow, and definitions of characteristic thickness \tilde{h} and velocity \tilde{u} . Reference heights of the Parcel, h_u and h_θ , are also shown.

For the steady state, drainage flow is governed by the following equations:

$$u' \frac{\partial u'}{\partial x} + w' \frac{\partial u'}{\partial z} = \frac{\partial}{\partial z} \left(\frac{\tau}{\rho} \right) + \frac{g\theta'}{\Theta_0} \sin \alpha, \quad (15)$$

$$u' \frac{\partial \theta'}{\partial x} + w' \frac{\partial \theta'}{\partial z} = - \frac{\partial}{\partial z} \left(\frac{H}{c_p \rho} \right) - \gamma u' \sin \alpha, \quad (16)$$

$$\frac{\partial u'}{\partial x} + \frac{\partial w'}{\partial z} = 0, \quad (17)$$

where τ and H are downward momentum and sensible heat fluxes, respectively. After integrating these equations vertically and transforming them, expressions for \tilde{h} and \tilde{u} can be derived.

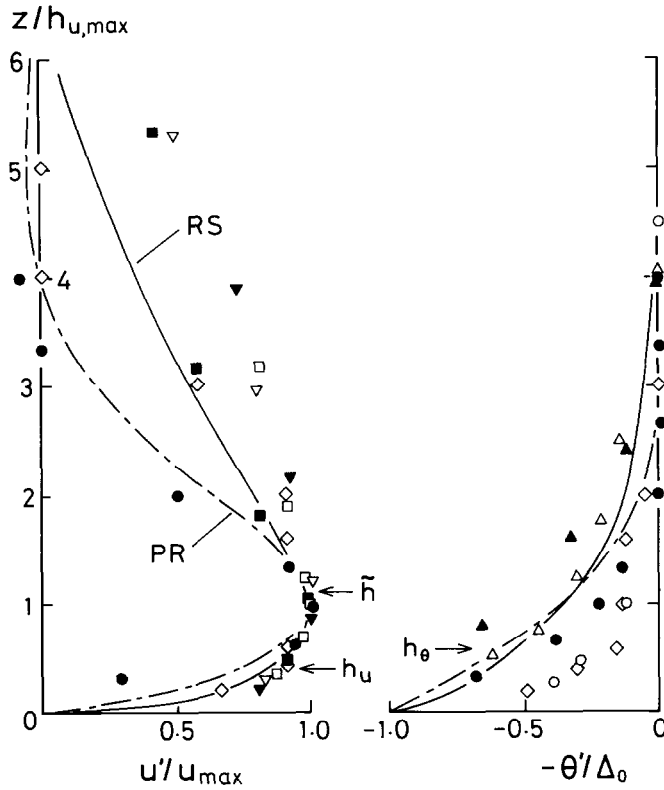


Fig. 3. Normalized profiles of velocity and potential temperature deviation. PR and RS denote the theoretical results of Prandtl (1952) and of Rao and Snodgrass (1981), respectively. Plots are the observations under calm conditions: \circ , ∇ , \blacktriangledown , Martin (1975); \bullet , Dickerson and Gudiksen (1983); \triangle , \blacktriangle , Clements and Nappo (1983); \square , \blacksquare , Ohata and Higuchi (1979); \diamond , Imaoka (1964).

For the transformations, several profile factors describing the distributions of potential temperature deviation and velocity of drainage flow are required. These factors were determined from the analytical solution (Prandtl, 1952) and from the numerical solution (Rao and Snodgrass, 1981) for a homogeneous and infinite slope. Hereafter these solutions are referred to as 'PR' and 'RS', respectively. Figure 3 shows the theoretical profiles of normalized velocity and of normalized potential temperature deviation together with the observations under calm conditions. The scale of potential temperature deviation Δ_0 is defined as the potential temperature difference between $z = h_{inv}$ and $z = 0$. Here h_{inv} is the height where $d\theta'/dz$ first tends to zero in the theoretical profiles, and the height where air temperature begins to deviate from ambient air temperature in the observed profiles. The height of maximum velocity is denoted by $h_{u,max}$. Though some scatter is seen, the observations are close to the theoretical profiles on average. The profile factors determined from PR and RS, and adopted in the present study are summarized in Table I. For simplification, we assume that these factors do not change along a slope.

TABLE I

Profile factors determined from Prandtl (1952) and Rao and Snodgrass (1981), and adopted in the present study

Definition	Prandtl	Rao and Snodgrass	Present study
$a_1 = \frac{1}{\tilde{h}} \int_0^{\infty} u' dz / \frac{1}{\tilde{h}} \int_0^{\tilde{h}} u' dz$	2.0	3.6	3.0
$a_2 = \frac{1}{\tilde{h}} \int_0^{\infty} \theta' u' dz / \left(\frac{1}{\tilde{h}} \int_0^{\infty} \theta' dz \frac{1}{\tilde{h}} \int_0^{\infty} u' dz \right)$	0.50	0.34	0.40
$a_3 = \frac{1}{\tilde{h}} \int_0^{\infty} u'^2 dz / \left(\frac{1}{\tilde{h}} \int_0^{\infty} u' dz \right)^2$	0.50	0.24	0.37
$a_4 = h_u / \tilde{h}$		0.36	0.36
$a_5 = h_\theta / \tilde{h}$		0.55	0.55
$a_6 = h_{inv} / \tilde{h}$	2.4	4.7	3.6
$a_7 = u_{max} / \tilde{u}$	1.3	1.2	1.3

With the profile factors, characteristic thickness and velocity of drainage flow are obtained. (See Appendix.) Characteristic thickness is expressed as

$$\tilde{h} = \frac{\frac{1}{3} C_H x}{1 + x/l_c}. \quad (18)$$

In the limits of $x \ll l_c$ and $x \gg l_c$,

$$\tilde{h} = \frac{1}{3} C_H x \quad (19a)$$

$$\tilde{h} = \tilde{h}_c = \frac{1}{3} C_H l_c \quad (\text{for } x \ll l_c), \quad (19a)$$

$$(\text{for } x \gg l_c). \quad (19b)$$

Characteristic velocity is expressed as

$$\tilde{u} = \left(\frac{\frac{1}{3} \frac{g\theta}{\Theta_0} \sin \alpha \frac{C_H}{C_M} \frac{1}{1 + \frac{5}{3} \frac{C_H}{C_M}} x \right)^{1/2} \quad (\text{for } x \leq l_c), \quad (20a)$$

$$\tilde{u} = \left(\frac{1}{3} \frac{g\theta}{\Theta_0} \sin \alpha \frac{C_H}{C_M} l_c \right)^{1/2} \times$$

$$\times \left[\frac{\frac{5}{3} \frac{C_H}{C_M}}{1 + \frac{5}{3} \frac{C_H}{C_M}} \exp \left\{ \frac{6}{5} \frac{C_M}{C_H} \left(1 - \frac{x}{l_c} \right) \right\} \right]^{1/2} \quad (\text{for } x > l_c).$$

In the limit of $x \gg l_c$,

$$\tilde{u} = \tilde{u}_c = \left(\frac{1}{3} \frac{g\theta}{\Theta_0} \sin \alpha \frac{C_H}{C_M} l_c \right)^{1/2} \quad (\text{for } x \gg l_c). \quad (20b)$$

In Equations (18)–(20), l_c is the equilibrium length of slope (Equation (12)) and x is the downslope distance from the crest.

According to PR and RS, the values of the profile factors a_6 and a_7 are determined as

$$a_6 = h_{\text{inv}}/\tilde{h} = 3.6, \quad (21)$$

$$a_7 = u_{\text{max}}/\tilde{u} = 1.3. \quad (22)$$

Substitution of the above values into Equations (19a), (20a), and (20b) yields

$$h_{\text{inv}} = 3.6\tilde{h} = 1.2C_H x, \quad (23)$$

$$1.3\tilde{u} = 0.78 \left(\frac{1}{2} \frac{g\theta}{\Theta_0} \sin \alpha \frac{C_H}{C_M} x \right)^{1/2} \quad (\text{for } x \ll l_c), \quad (24a)$$

$u_{\text{max}} =$

$$1.3\tilde{u}_c = 1.06 \left(\frac{1}{2} \frac{g\theta}{\Theta_0} \sin \alpha \frac{C_H}{C_M} l_c \right)^{1/2} \quad (\text{for } x \gg l_c). \quad (24b)$$

In the transformation of Equation (20a) into Equation (24a), an approximation of $\frac{5}{3}C_H/C_M \simeq \frac{5}{3} \times 0.5$ is used.

Under the assumption that the mean bulk coefficients based on the velocity of the Parcel (Section 2.2) and those based on the characteristic velocity of drainage flow are the same, comparisons of the thickness and velocity of the Parcel (h and u , Equations (5a) and (10)) with those of drainage flow (h_{inv} and u_{max} , Equations (23) and (24)) yield the following relations:

$$h_{\text{inv}} = 1.2h, \quad (25)$$

$$u_{\text{max}} = \begin{cases} 0.78u & (\text{for } x \ll l_c), \\ 1.06u_c & (\text{for } x \gg l_c). \end{cases} \quad (26a)$$

$$(26b)$$

Roughly speaking, the above three equations show that the thickness of the Parcel h corresponds to h_{inv} , the velocity of the Parcel u corresponds to u_{max} , and $u \simeq \tilde{u}$. These approximations will be used in Section 3.2, where the Parcel Model will be compared with observations.

The flow rate and longitudinal heat flux (negative heat flux relative to the ambient atmosphere) associated with drainage flow are expressed with the profile factors a_1 and a_2 as

$$\text{flow rate: } q^* = \int_0^{\infty} u' dz = a_1 \tilde{h} \tilde{u} = 3 \tilde{h} \tilde{u}, \quad (27)$$

$$\begin{aligned} \text{longitudinal heat flux: } H^* &= c_p \rho \int_0^{\infty} \theta' u' dz = a_1 a_2 c_p \rho \tilde{h} \theta \tilde{u} \\ &= 1.1 c_p \rho \tilde{h} \theta \tilde{u}. \end{aligned} \quad (28)$$

2.5. MEAN BULK COEFFICIENTS, C_H AND C_M

The definitions of the mean bulk coefficients of the Parcel, C_H and C_M , are somewhat different from those of C_h and C_m ordinarily used in the horizontal surface layer. For so-called 'log' profiles, C_h and C_m are written as

$$C_h = \frac{k^2}{\ln \frac{z_r}{z_0} \ln \frac{z_r}{z_\theta}}, \quad C_m = \frac{k^2}{\left(\ln \frac{z_r}{z_0} \right)^2}, \quad (29)$$

where k ($= 0.4$) is the von Kármán constant, z_r the reference height, and z_0 and z_θ the roughness lengths for the velocity and potential temperature profiles, respectively.

In the first place, the 'local' bulk coefficients, C_H^* and C_M^* , are determined. The local fluxes of sensible heat H_0 and momentum τ_0 at a certain location on the slope, where the thickness and velocity of the Parcel are h and u (characteristic thickness and velocity of drainage flow are \tilde{h} and \tilde{u}), respectively, are expressed as

$$\frac{H_0}{c_p \rho} = u_* \theta_* = C_H^* u \theta, \quad (30)$$

$$\frac{\tau_0}{\rho} = u_*^2 = C_M^* u^2. \quad (31)$$

The heights h_u and h_θ , where the velocity and potential temperature deviation are equal to u and θ , respectively, are adopted as the reference heights of the Parcel (see Figures 2 and 3). With the profile factors, $a_4 = h_u/\tilde{h} = 0.36$, $a_5 = h_\theta/\tilde{h} = 0.55$, and $a_6 = h_{\text{inv}}/\tilde{h} = 3.6$, the result is obtained that

$$\frac{h_u}{h} \simeq \frac{h_u}{h_{\text{inv}}} = \frac{a_4}{a_6} = 0.10, \quad \frac{h_\theta}{h} \simeq \frac{h_\theta}{h_{\text{inv}}} = \frac{a_5}{a_6} = 0.15. \quad (32)$$

Assuming so-called 'log + linear' profiles below the levels of h_u and h_θ in the drainage flow, one may express the local bulk coefficients as

$$C_H^* = \frac{k^2}{\left(\ln \frac{h_u}{z_0} + \beta \frac{h_u}{L} \right) \left(\ln \frac{h_\theta}{z_\theta} + \beta \frac{h_\theta}{L} \right)}, \quad C_M^* = \frac{k^2}{\left(\ln \frac{h_u}{z_0} + \beta \frac{h_u}{L} \right)^2}. \quad (33)$$

The terms including β ($\simeq 7$) represent the effect of stability. With Equations (30) and (31), the Monin–Obukhov length L is written as

$$L = \frac{C_M^{*3/2} u^2}{k \frac{g}{\Theta_0} C_H^* \theta}. \quad (34)$$

With the relations $C_H^* = \frac{2}{3} C_H$ and $C_M^* = \frac{2}{3} C_M$ (shown later), Equations (5a), (10a), (32),

and (34) yield

$$\beta \frac{h_u}{L} = \frac{0.7k(1 + F_5)}{\sqrt{\frac{2}{3}}} \frac{C_H}{C_M} \frac{\sqrt{C_M}}{\sin \alpha} = 0.7 \frac{C_H}{C_M} \frac{\sqrt{C_M}}{\sin \alpha}, \quad (35)$$

and

$$\beta \frac{h_\theta}{L} = 1.1 \frac{C_H}{C_M} \frac{\sqrt{C_M}}{\sin \alpha}. \quad (36)$$

These stability-dependent terms may be neglected for ordinary slopes except for the case where C_M is very large or α is very small. Thus the local bulk coefficients can be expressed as

$$C_H^* = \frac{k^2}{\ln \frac{0.10h}{z_0} \ln \frac{0.15h}{z_\theta}}, \quad C_M^* = \frac{k^2}{\left(\ln \frac{0.10h}{z_0} \right)^2}. \quad (37)$$

Next, the mean bulk coefficient for heat exchange C_H for a slope of length l is determined. Substitution of Equation (30) into Equation (4) yields

$$C_H(l) = \frac{\langle H_0 \rangle / (c_p \rho)}{\theta \langle u \rangle} = \frac{1}{l} \int_0^l C_H^*(x) \frac{u(x)}{\langle u \rangle} dx, \quad (38)$$

which indicates that C_H is a mean of C_H^* weighted by $u/\langle u \rangle$. Though the dependence of u on x varies with ambient stability, the following approximate equation was found regardless of γ :

$$C_H(l) \simeq \frac{3}{2} C_{H0}^*(l), \quad (39)$$

where C_{H0}^* is the local bulk coefficient given by Equation (37) under neutral ambient stratification. The mean bulk coefficient for momentum exchange C_M is expressed as

$$\langle \tau_0 \rangle / \rho = C_M \langle u \rangle^2. \quad (40)$$

Substitution of Equation (31) into Equation (40) yields

$$C_M(l) = \frac{\langle \tau_0 \rangle / \rho}{\langle u \rangle^2} = \frac{1}{l} \int_0^l C_M^*(x) \frac{u^2(x)}{\langle u \rangle^2} dx. \quad (41)$$

This indicates that C_M is a mean of C_M^* weighted by $u^2/\langle u \rangle^2$. An approximation similar to Equation (39), however, is also adopted for C_M . Equations (5a), (37), and (39) yield

$$C_H(l) = \frac{\frac{3}{2}k^2}{\ln \frac{0.10C_H(l)l}{z_0} \ln \frac{0.15C_H(l)l}{z_\theta}},$$

$$C_M(l) = \frac{\frac{3}{2}k^2}{\left(\ln \frac{0.10C_H(l)l}{z_0} \right)^2}. \quad (42)$$

Equation (42) shows that the mean bulk coefficients are functions of slope length as well as roughness lengths. The relations between the local and mean bulk coefficients are given by

$$C_{H, M}^*(x) = \begin{cases} \frac{2}{3}C_{H, M}(x) & (x \leq l_c), \\ \frac{2}{3}C_{H, M}(l_c) & (x > l_c). \end{cases} \quad (43)$$

Figure 4 represents the mean bulk coefficients, C_H and C_M , versus slope length l (lower figure) and the ratio C_H/C_M versus l (upper). In the figure, the 'rough' surface refers to a surface covered with trees or grass ($z_0 = 31.6$ cm and $z_\theta = 1$ cm), and the 'smooth' surface to a flat snow surface ($z_0 = z_\theta = 0.01$ cm). The mean bulk coefficients decrease with l because the reference heights of the Parcel, which are proportional to its thickness, increase with l .

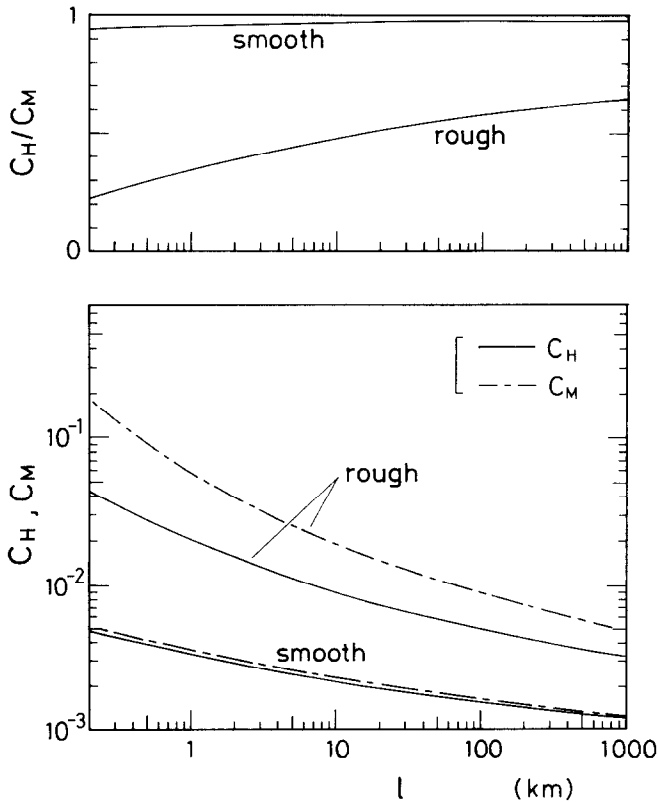


Fig. 4. Relations between mean bulk coefficients, C_H and C_M , and slope length l (lower figure), and those between C_H/C_M and l (upper). The 'rough' and 'smooth' surfaces are covered with trees or grass and smooth snow, respectively.

3. Discussion

3.1. COMPARISON WITH PREVIOUS THEORETICAL WORKS

Earlier theoretical works of Defant (1933) and Reiher (1936) did not consider the thermodynamics of drainage flow. Reiher derived an expression for velocity in which drainage flow was regarded as the sinking of cold air due to gravity. Defant adopted the idea that the gravitational force is balanced by the frictional force. If the thickness in Defant's expression for the velocity is given by Equation (5a), his result coincides with our Equation (10a) for neutral ambient stratification.

Manins and Sawford (1979)(MS) proposed a hydraulic model, in which they included a pressure gradient force and an interfacial drag and assumed that the sum of sensible and radiative heat loss is constant along the slope. In our Parcel Model (PM), however, the pressure gradient force and radiative heat loss are neglected; interfacial drag is parameterized with F_5 ; and sensible heat is expressed through the use of C_H .

Though the definitions and assumptions are different between PM and MS, we can examine qualitative dependencies of the following two quantities on the downslope distance x :

$$\begin{aligned} \text{flow rate} &\propto \int_0^{\infty} u' dz \propto \begin{cases} hu & \text{(PM),} \\ h_{MS}u_{MS} & \text{(MS),} \end{cases} \\ \text{heat deficit} &\propto \int_0^{\infty} \theta' dz \propto \begin{cases} h & \text{(PM),} \\ h_{MS}\Delta_{MS} & \text{(MS).} \end{cases} \end{aligned} \quad (44)$$

3.1.1. Neutral Ambient Stratification

Under the assumption of constant C_H and C_M , PM and MS show somewhat different dependencies as follows:

$$\begin{aligned} \text{flow rate} &\propto \begin{cases} x^{3/2} & \text{(PM),} \\ x^{4/3} & \text{(MS),} \end{cases} \\ \text{heat deficit} &\propto \begin{cases} x & \text{(PM),} \\ x^{2/3} & \text{(MS).} \end{cases} \end{aligned} \quad (45)$$

3.1.2. Stable Ambient Stratification

According to MS, the flow rate and heat deficit increase with x but the latter has a maximum under certain conditions. PM shows, however, that both increase monotonically and attain equilibrium values. Under the equivalent assumptions to MS on diabatic cooling, PM's dependence of the heat deficit on x agrees with MS's, but that of the flow rate on x does not (Sato and Kondo, 1985a).

3.2. COMPARISON WITH OBSERVATIONS

3.2.1. Mean Bulk Coefficients

In order to determine C_H and C_M observationally, it is necessary to know the sensible heat and momentum fluxes as well as the temperature and velocity distributions of drainage flow. Many investigators have been interested in the overall structure of drainage flow, but only a few flux measurements have been made. Here we use available data of the katabatic wind at Mizuho Station, Antarctica, and the data taken on the simple slope several hundred meters long.

Firstly, four cases under typical katabatic wind conditions (strong surface inversion is present, maximum velocity exists, and ambient velocity at a height of 1 km is less than 10 m s^{-1}) are analyzed. The characteristics of drainage flow, u_{\max} and θ , were determined from the low-level radiosonde data by Kawaguchi *et al.* (1985), and the sensible heat and momentum fluxes were calculated from the temperature and velocity profiles measured with 30 m tower by Ohata *et al.* (1983). With Equations (30), (31), and (43), $C_H = 0.7 \times 10^{-3}$ and $C_M = 2 \times 10^{-3}$ are obtained, which do not differ greatly from the theoretical values for the 'smooth' surface with $l = 300 \text{ km}$ (Figure 4).

Secondly, observational results on Rattlesnake Mountain (Horst and Doran, 1986) are examined. They obtained $C_d = 0.034\text{--}0.041$, where $\tau_0/\rho = C_d U^2$ and U is defined in the same way as Manins and Sawford (1979). Considering that their surface stress is a local value and that $U/u \simeq 0.7$ (according to PR and RS), $C_M^* = 0.017\text{--}0.021$ and, hence, $C_M = 0.026\text{--}0.032$ are obtained. This value of C_M almost agrees with the theoretical value for their slope conditions ($l = 400\text{--}1000 \text{ m}$ and $z_0 = 3 \text{ cm}$).

3.2.2. Thickness and Velocity of Drainage Flow

Comparisons are made between the present Parcel Model and the observations under weak ambient winds. Table II summarizes the observed values from the literature where most of the governing parameters are reported. The governing parameters are the slope length l , vertical drop δz (both are measured from the crest), potential temperature difference between the ambient atmosphere and drainage flow θ , ambient potential temperature gradient γ , and slope surface condition. In the table, h_{inv} is the observed inversion height, u_{\max} the maximum velocity, and $h_{u, \max}$ the height of maximum velocity.

In Figure 5(a), observed values of the thickness of drainage flow versus slope length are plotted. The smaller of the l and l_c values was used; however, when γ was not known, the topographic value l was used provisionally. Since h_{inv} was not observed for No. 1, $2.8h_{u, \max}$ was used instead. The factor 2.8 is the mean value of the ratio $h_{\text{inv}}/h_{u, \max}$ calculated from the listed data in Table II. The solid lines are the theoretical values of h for the 'rough' and 'smooth' surfaces, whose definitions were given in Section 2.5. The broken lines are the theoretical values (Equation (5a)) for $C_H = 0.001$ and $C_H = 0.01$. Note that the value of C_H decreases with slope length.

The observed values of Nos. 6, 7, and 12 are slightly smaller than the theoretical ones for the 'rough' surface. This may be attributed to their surface conditions: their slopes are covered with grass or small shrubs; consequently the value of C_H is smaller than

TABLE II

Characteristics of drainage flows observed on simple slopes and governing parameters. The parentheses indicate estimated maximum velocity, a blank indicates that the value was not observed. Data are from the following literature: (1) Ohata and Higuchi (1979), (2) Martin (1975), (3) Ohata *et al.* (1984), (4) Adachi and Kawaguchi (1984), (5) Adachi (1983), (6, 13) Sato and Kondo (1985b), (7) Clemens and Nappo (1983), (8) Imaoka (1964), (9) Dickerson and Gudiksen (1983), (10) Tanaka *et al.* (1982, 1983), (11) Kondo and Kuwagata (1984), (12) Kudo *et al.* (1982), (14) Banta and Cotton (1981), (15) Dohkoshi *et al.* (1985).

No.	Observation site	l (km)	δz (km)	θ ($^{\circ}\text{C}$)	γ ($^{\circ}\text{C km}^{-1}$)	h_{inv} (m)	$h_{e, \text{max}}$ (m)	u_{max} (m s^{-1})	Notes
(Snow or glacier)									
1	Mt. Tsurugi	0.78	0.30				1.1		Small snow patch, Period 1
		0.25	0.04	4.0-6.4			0.7	1.4-2.2	Small snow patch, Period 2
2	Glacier de St-Sorlin	2.5	0.31	2.0-6.6		4	2	1.4-4.4	Glacier, 3-day mean
3	Glacier San Rafael	40	2.8	3.5		100	50	5	Glacier
4	Mizuho Station	300	0.77	7.2	5	325	50	14	Antarctica, mean of 26 obs.
5	Syowa Station	550	3.0	3.8	1	400	200	15.4	Antarctica, mean of 14 obs.
(Trees or grass)									
6	Mt. Azuma ko-Fuji	0.037-0.089 0.068-0.095	0.020-0.043 0.034-0.048	0.5-2.7 0.3-2.5	6-105 13-46	1.6-3.5		(0.3-1.0)	Grass Grass
7	Pajarito Mountain	0.092	0.046	2.9-4.1	20-69			(0.7-1.0)	Gravel Grass, upper mast Grass, lower mast
		0.30	0.06	2.5		5		(2.5)	Trees and grass
8	Hakatajima	0.82	0.25	3.0		15	5	2.4	Trees and grass, Unit-19
9	Cobb Mountain	0.69	0.15	2.0		15	15	1.2	Sparse trees and snow, mean of 7 obs.
10	Tomakomai	2.4 17	0.45 0.33	5.0 10.0	2	40 88	40 88	(3)	Trees, mean of 10 obs. Grass
11	Sendai	34	1.1	3.5	4	280		(4)	Trees and grass
12	Sugadaira	1.0-1.5	0.28-0.33	3.1-3.4	24	5-8			Trees and grass
13	Kawatani	1.8	0.33	1.6-2.5	1-16	18-28		3	Trees
14	South Park	18	1.4	3.7	19	38	25		
15	Hayakita	5.2	0.11	3.5	3	60			

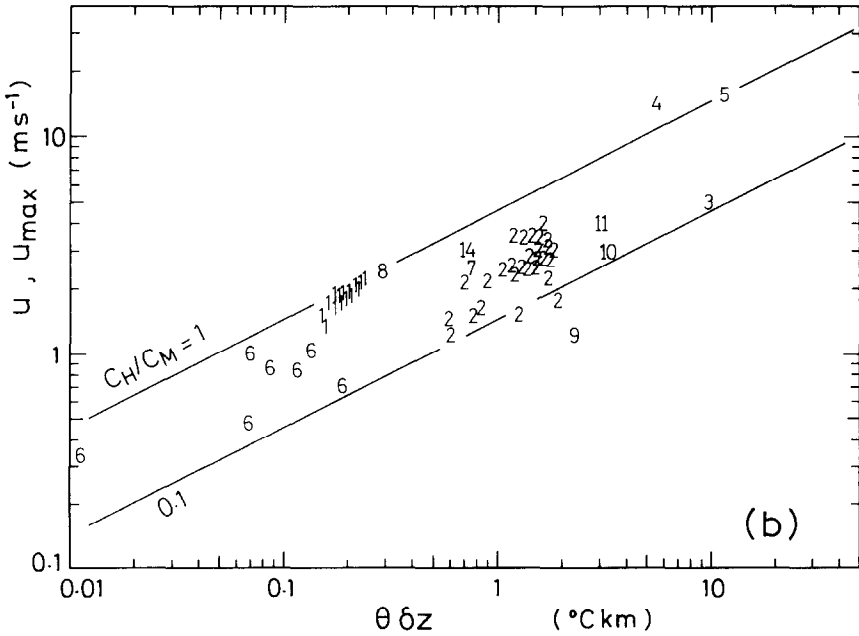
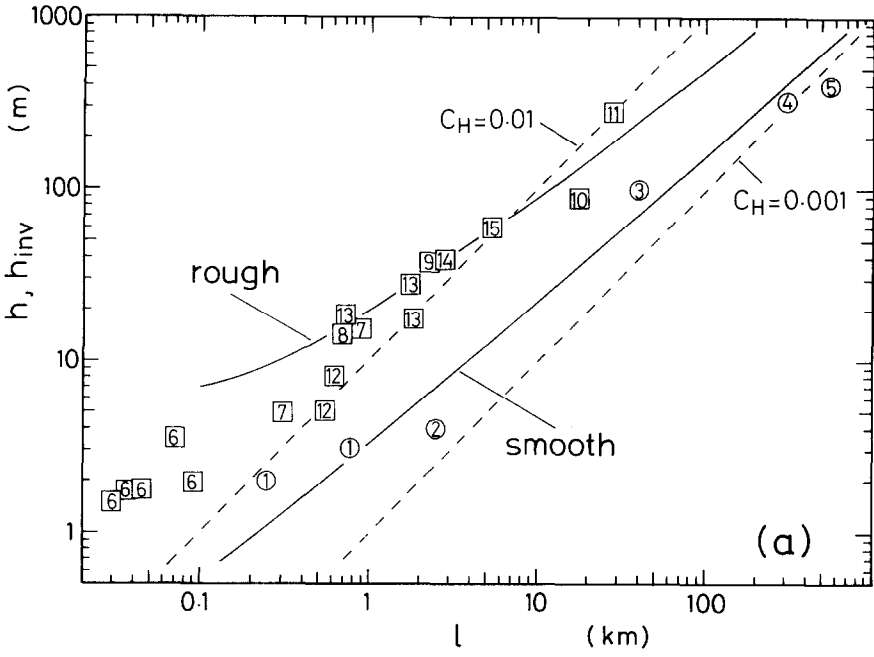


Fig. 5. Relation between the thickness of drainage flow and slope length (a) and that between the velocity and $\theta \delta z$ (b). Solid and broken lines represent the predictions by the Parcel Model. Observations are plotted with the numerals indicating observation sites (Table II). Symbols indicate types of slope surfaces (circle: snow or glacier surface, square: trees or grass-covered surface).

that for the 'rough' surface. Figure 5(a) shows agreement between the Parcel Model and observations over a wide range of slope lengths. The dependence of the thickness of drainage flow on the aerodynamic roughness is also consistent with the Parcel Model.

Figure 5(b) shows the velocity of drainage flow versus $\theta \delta z$, in which numerals indicate observation sites and the smaller value between δz and $l_c \sin \alpha$ is used when γ is known. The solid lines are the theoretical values of u (Equation (10a)) for $C_H/C_M = 0.1$ and $C_H/C_M = 1$. Instead of θ , the temperature difference between $z = 2.4$ m and $z = 0.4$ m for No. 1, and that between $z = 9.5$ m and $z = 0.5$ m for No. 2 are used.

The observed velocities of Nos. 4 and 5 may be larger than those expected under calm conditions because of the ambient winds which may accelerate the drainage flows. The Coriolis force cannot be neglected for large-scale drainage flow such as the katabatic wind (Nos. 4 and 5). Incorporating the Coriolis force, Kondo (1984) obtained the velocities 0.75 (No. 4) and 0.96 (No. 5) of those when the Coriolis force was neglected.

4. Conclusions

A simple model of drainage flow on a slope (Parcel Model) has been proposed. The model is based on the momentum and sensible heat transports to the slope surface under calm conditions. The main conclusions are as follows:

(1) With the concept of a cold air 'Parcel' together with its heat budget and equation of motion, the thickness h and velocity u of the Parcel have been derived in simple forms. The governing parameters for h and u are the length and vertical drop of the slope, potential temperature difference between the ambient atmosphere and the Parcel, and the aerodynamic condition of the slope surface expressed by the mean bulk coefficients. The influence of ambient stratification on drainage flow is represented by the 'equilibrium length of slope'.

(2) With several profile factors, h and u of the Parcel were shown to correspond to the inversion height h_{inv} and maximum velocity u_{max} of an actual drainage flow, respectively. The flow rate and longitudinal heat flux associated with drainage flow were formulated.

(3) The mean bulk coefficients of the Parcel were determined under some assumptions on the form of the temperature and velocity profiles of drainage flow. They are expressed in terms of roughness lengths (z_0 and z_θ) and a slope length.

(4) The Parcel Model agrees qualitatively with the hydraulic model of Manins and Sawford (1979) when ambient stratification is neutral. Under stable conditions, agreement is not so good.

(5) The thickness and velocity of drainage flow predicted by the Parcel Model agree with observations on slopes several tens of meters to several hundred kilometers long.

Since the Parcel Model is rather simple, it may be useful for the study of energy exchange over complex terrain, and for the prediction of the development of cold-air pools or an inland local high pressure area.

Acknowledgments

We are grateful to Dr N. Yasuda of Meteorological College and Professor W. H. Brutsaert of Cornell University for valuable discussions and comments. This study was supported by a Fund for Scientific Research from the Ministry of Education, Science and Culture of Japan.

Appendix. Derivations of Characteristic Thickness and Velocity of Drainage Flow

Characteristic thickness and velocity of drainage flow are derived as follows:

A.1. THICKNESS, \tilde{h}

Equations (16) and (17) yield

$$\frac{\partial \theta' u'}{\partial x} + \frac{\partial \theta' w'}{\partial z} = -\frac{\partial}{\partial z} \left(\frac{H}{c_p \rho} \right) - \gamma u' \sin \alpha. \quad (\text{A1})$$

After integration over z from zero to infinity, Equation (A1) results in

$$\frac{\partial}{\partial x} \int_0^\infty \theta' u' dz = \frac{H_0}{c_p \rho} - \gamma \sin \alpha \int_0^\infty u' dz, \quad (\text{A2})$$

where $w' = 0$ and $H = H_0$ at $z = 0$, and $w' = H = 0$ at $z = \infty$, in which H_0 denotes the sensible heat flux at the surface. With the profile factors a_1 and a_2 , Equation (A2) is rewritten as

$$\frac{\partial}{\partial x} (1.1 \tilde{h} \theta \tilde{u}) = \frac{H_0}{c_p \rho} - \gamma \sin \alpha \times 3 \tilde{h} \tilde{u}. \quad (\text{A3})$$

Integrating Equation (A3) over x' from zero to x with $\tilde{h} = 0$ at $x' = 0$, we obtain

$$1.1 \tilde{h}(x) \theta \tilde{u}(x) = \frac{x \langle H_0 \rangle}{c_p \rho} - 3 \gamma \sin \alpha \int_0^x \tilde{h} \tilde{u} dx', \quad (\text{A4})$$

where

$$\langle H_0 \rangle = c_p \rho C_H \langle \tilde{u} \rangle \theta. \quad (\text{A5})$$

The angular brackets denote the mean value over the interval $0-x$. The expression of $\langle H_0 \rangle$ is formally the same as Equation (4). For simplification, the following approximations are used:

$$\int_0^x \tilde{h} \tilde{u} dx' \simeq x \tilde{h}(x) \langle \tilde{u} \rangle, \quad (\text{A6})$$

$$1.1 \tilde{u}(x) \simeq 3 \langle \tilde{u} \rangle. \quad (\text{A7})$$

Then, Equation (A4) is rewritten as

$$\tilde{h}(x)(\theta + \gamma x \sin \alpha) \frac{3 \langle \tilde{u} \rangle}{x} = C_H \theta \langle \tilde{u} \rangle, \quad (\text{A8})$$

and we obtain

$$\tilde{h} = \frac{\frac{1}{3} C_H x}{1 + x/l_c}. \quad (\text{18})$$

A.2. VELOCITY, \tilde{u}

Equations (15) and (17) yield

$$\frac{\partial u'^2}{\partial x} + \frac{\partial u' w'}{\partial z} = \frac{\partial}{\partial z} \left(\frac{\tau}{\rho} \right) + \frac{g \theta'}{\Theta_0} \sin \alpha. \quad (\text{A9})$$

After integration over z from zero to infinity, Equation (A9) results in

$$\frac{\partial}{\partial x} \int_0^\infty u'^2 dz = -\frac{\tau_0}{\rho} + \tilde{h} \frac{g \theta}{\Theta_0} \sin \alpha, \quad (\text{A10})$$

where $\tau = \tau_0$ at $z = 0$ and $\tau = 0$ at $z = \infty$, in which τ_0 denotes the momentum flux at the surface. With the profile factors a_1 and a_3 , Equation (A10) is rewritten as

$$\frac{5}{2} \frac{\partial}{\partial x} (\tilde{h} \tilde{u}^2) = -\frac{\tau_0}{\rho} + \tilde{h} \frac{g \theta}{\Theta_0} \sin \alpha, \quad (\text{A11})$$

where

$$\tau_0/\rho = C_M \tilde{u}^2. \quad (\text{A12})$$

Substitution of Equation (A12) into Equation (A11) yields

$$\tilde{h} \frac{\partial \tilde{u}^2}{\partial x} = \frac{2}{5} \left\{ \tilde{h} \frac{g \theta}{\Theta_0} \sin \alpha - \left(C_M + \frac{5}{2} \frac{\partial \tilde{h}}{\partial x} \right) \tilde{u}^2 \right\}. \quad (\text{A13})$$

Considering that $\partial \tilde{u}^2/\partial x = 2 \tilde{u} \partial \tilde{u}/\partial x = 2 d\tilde{u}/dt$, Equation (A13) corresponds to the equation of motion of the Parcel (Equation (6)). The factor $\frac{2}{5}$ is caused by the shapes of the potential temperature deviation and the velocity distributions. Instead of the frictional force at the interface between the Parcel and the ambient atmosphere, the drag due to the change in characteristic thickness appears in Equation (A13). This term has the same effect as the drag due to entrainment.

Using Equation (19) with the assumption of constant C_H and C_M , we can obtain the analytical solutions of Equation (A13):

$$\tilde{u} = \left(\frac{1}{3} \frac{g \theta}{\Theta_0} \sin \alpha \frac{C_H}{C_M} \frac{1}{1 + \frac{5}{3} \frac{C_H}{C_M}} x \right)^{1/2} \quad (\text{for } x \leq l_c), \quad (\text{20a})$$

$$\tilde{u} = \left(\frac{1}{3} \frac{g\theta}{\Theta_0} \sin \alpha \frac{C_H l_c}{C_M} \right)^{1/2} \times \left[1 - \frac{\frac{5}{3} \frac{C_H}{C_M}}{1 + \frac{5}{3} \frac{C_H}{C_M}} \exp \left\{ \frac{6}{5} \frac{C_M}{C_H} \left(1 - \frac{x}{l_c} \right) \right\} \right]^{1/2} \quad (\text{for } x > l_c), \quad (20c)$$

where $\tilde{u} = 0$ at $x = 0$ for $x \leq l_c$, and \tilde{u} at $x = l_c$ is given by Equation (20a) for $x > l_c$. The exponential part on the right-hand side of Equation (20c) represents the transitional form of the velocity for $x > l_c$ before reaching its equilibrium value. Since the solutions of Equation (A13) under the assumption of $\partial \tilde{u}^2 / \partial x = 0$ do not differ much from Equations (20a) and (20c), the approximation in Section 2.2 is adequate.

References

- Adachi, T.: 1983, *Numerical Simulation of Strong Katabatic Winds at Syowa and Mizuho Stations, Antarctica*, Mem. Natl. Inst. Polar Res., Spec. Issue, No. 29, pp. 50–60.
- Adachi, T. and Kawaguchi, S.: 1984, *Numerical Simulation of Katabatic Wind at Mizuho Station, East Antarctica*, Mem. Natl. Inst. Polar Res., Spec. Issue, No. 34, pp. 37–53.
- Atkinson, B. W.: 1981, *Meso-Scale Atmospheric Circulations*, Academic Press, New York, 495 pp.
- Banta, R. and Cotton, W. R.: 1981, 'An Analysis of the Structure of Local Wind Systems in a Broad Mountain Basin', *J. Appl. Meteorol.* **20**, 1255–1266.
- Briggs, G. A.: 1981, 'Canopy Effects on Predicted Drainage Flow Characteristics and Comparisons with Observations', preprint volume of extended abstracts: Fifth Symposium on Turbulence, Diffusion, and Air Pollution, pp. 113–115.
- Clements, W. E. and Nappo, C. J.: 1983, 'Observations of a Drainage Flow Event on a High-Altitude Simple Slope', *J. Climate Appl. Meteorol.* **22**, 331–335.
- Defant, A.: 1933, 'Der Abfluss schwerer Luftmassen auf geneigtem Boden, nebst einigen Bemerkungen zur Theorie stationärer Luftströme', *Sitz. Ber. Preuss. Akad. Wiss. (Phys. Math. Klasse)* **18**, 624–635.
- Dickerson, M. H. and Gudiksen, P. H. (eds.): 1983, *Atmospheric Studies in Complex Terrain*, Tech. Progress Rep. 1979–1983, ASCOT 84-1, Lawrence Livermore National Lab. Univ. of California, 376 pp.
- Dohkoshi, J., Horiguchi, I., and Tani, H.: 1985, *An Observational Study on the Nocturnal Cooling at Hayakita and Oiwake, Hokkaido*, Rep. Spec. Res. Proj. Natural Disaster, No. A-60-4, pp. 167–178 (in Japanese).
- Fitzjarrald, D. R.: 1984, 'Katabatic Wind in Opposing Flow', *J. Atmos. Sci.* **41**, 1143–1158.
- Garrett, A. J.: 1983, 'Drainage Flow Prediction with a One-Dimensional Model Including Canopy, Soil and Radiation Parameterizations', *J. Climate Appl. Meteorol.* **22**, 79–91.
- Gutman, L. N.: 1983, 'On the Theory of the Katabatic Slope Wind', *Tellus* **35A**, 213–218.
- Horst, T. W. and Doran, J. C.: 1986, 'Nocturnal Drainage Flow on Simple Slopes', *Boundary-Layer Meteorol.* **34**, 263–286.
- Imaoka, E.: 1964, 'Relation Between Down Slope Wind and General Wind', *J. Agric. Meteorol.* **20**, 41–45 (in Japanese with English summary).
- Kawaguchi, S., Kobayashi, S., Ishikawa, N., Ohata, T., Inoue, J., Satow, K., and Nishimura, H.: 1985, *Aerological Sounding of Lower Atmospheric Layer over Mizuho Plateau, East Antarctica*, JARE Data Rep., No. 104, 128 pp.
- Kondo, J.: 1984, 'Effect of the Topographical and Ground Surface Conditions on the Nocturnal Drainage Wind and Cooling in Mountainous Regions (Part 1)', *Tenki* **31**, 625–632 (in Japanese).
- Kondo, J. and Kuwagata, T.: 1984, 'A Relation Between the Depth of Nocturnal Stable Layer (Cold-Air-Pool) and the Topographical Depth of the Basin', *Tenki* **31**, 727–737 (in Japanese).
- Kudo, T., Tanaka, H., Toritani, H., and Hwang, S.: 1982, 'Formation of Cold Air Lake in Sugadaira Basin', *Geogr. Rev. Japan* **55**, 849–856 (in Japanese with English abstract).

- Manins P. C. and Sawford, B. L.: 1979, 'A Model of Katabatic Winds', *J. Atmos. Sci.* **36**, 619–630.
- Martin, S.: 1975, 'Wind Regimes and Heat Exchange on Glacier de Saint Sorlin', *J. Glaciol.* **14**, 91–105.
- Ohata, T. and Higuchi, K.: 1979, 'Gravity Wind on a Snow Patch', *J. Meteorol. Soc. Japan* **57**, 254–263.
- Ohata, T., Ishikawa, N., Kobayashi, S., and Kawaguchi, S.: 1983, *Micro-Meteorological Data at Mizuho Station, Antarctica in 1980*, JARE Data Rep., No. 79, 374 pp.
- Ohata, T., Kondo, H., and Enomoto, H.: 1984, 'Drainage Flow Observed on Glacier San Rafael', *Proceedings of 1984 Spring Convention Japan Meteorol. Soc.* **45**, 95 (in Japanese).
- Prandtl, L.: 1952, *Essentials of Fluid Dynamics*, Blackie and Son Ltd., London and Glasgow, 452 pp.
- Rao, P. K. and Snodgrass, H. F.: 1981, 'A Nonstationary Nocturnal Drainage Flow Model', *Boundary-Layer Meteorol.* **20**, 309–320.
- Reiher, M.: 1936, 'Nächtlicher Kaltluftfluss an Hindernissen', *Bioklim. Beiblätter (Braunschweig)* **3**, 152–163.
- Sato, T. and Kondo, J.: 1985a, *Modeling of the Nocturnal Drainage Wind (Part 1)*, Rep. Spec. Res. Proj. Natural Disaster, No. A-60-4, pp. 349–368 (in Japanese).
- Sato, T. and Kondo, J.: 1985b, *Modeling of the Nocturnal Drainage Wind (Part 2)*, Rep. Spec. Res. Proj. Natural Disaster, No. A-60-4, pp. 369–386 (in Japanese).
- Tanaka, Y., Fujiwara, K., and Kobayashi, D.: 1983, 'Nocturnal Cooling in the Shallow Valley and on the Plateau, (2) Topographical Dependence of Cooling Process', *J. Agric. Meteorol.* **39**, 213–217 (in Japanese with English summary).
- Tanaka, Y., Ishigaki, K., Fujiwara, K., and Kobayashi, D.: 1982, 'Nocturnal Cooling in the Shallow Valley and on the Plateau, (1) Cooling Process in the Valley and on the Side Slope', *J. Agric. Meteorol.* **38**, 245–251 (in Japanese with English summary).
- Yamada, T.: 1981, 'A Numerical Simulation of Nocturnal Drainage Flow', *J. Meteorol. Soc. Japan* **59**, 108–122.
- Yamada, T.: 1983, 'Simulations of Nocturnal Drainage Flows by a q^2 Turbulence Closure Model', *J. Atmos. Sci.* **40**, 91–106.